APPLIED PHYSICS LETTERS **105**, 072403 (2014)

CrossMark

533

Exchange bias: The antiferromagnetic bulk matters

Ali C. Basaran,[1,2,a)] T. Saerbeck,[1] J. de la Venta,[3] H. Huckfeldt,[4] A. Ehresmann,[4] and Ivan K. Schuller[1]
[1]*Department of Physics and Center for Advanced Nanoscience, University of California San Diego, La Jolla, California 92093, USA*
[2]*Materials Science and Engineering, University of California San Diego, La Jolla, California 92093, USA*
[3]*Department of Physics, Colorado State University, Fort Collins, Colorado 80523, USA*
[4]*Institute of Physics and Center for Interdisciplinary Nanostructure Science and Technology (CINSaT), University of Kassel, Heinrich-Plett-Str. 40, 34132 Kassel, Germany*

(Received 26 May 2014; accepted 7 August 2014; published online 18 August 2014)

Using controlled ion bombardment, the contribution of interface and bulk antiferromagnetic spins to exchange bias (EB) is investigated. Several sets of ferromagnetic (FM)/antiferromagnetic (AFM) (Ni/FeF_2) bilayers capped with a nonmagnetic and inert Au layer of varying thickness were grown simultaneously. He-ion bombardment was employed to selectively create defects in the EB structure at the FM/AFM interface or in the AFM bulk. Numerical simulations provide the depth profile of the ion damage. Quantitative structural and magnetic characterizations were compared before and after the bombardment revealing the relationship between interfacial and bulk located defects. These studies show that the creation of defects in the bulk of the antiferromagnet crucially affects the magnitude of EB. © *2014 AIP Publishing LLC*. [http://dx.doi.org/10.1063/1.4893457]

Although the application of exchange bias (EB) is well established in the current sensor[1,2] and storage[3] technologies and is of a great importance in the design of new spintronic devices,[4–6] the contribution of the magnetic structure in the antiferromagnetic bulk is still ambiguous. EB is defined as a unidirectional anisotropy due to exchange coupling between two magnetic materials.[7] Therefore, EB is generally assumed to be an interfacially governed property.[8,9] Consequently, most attempts of tailoring the effect in magnitude or direction are based on control of the magnetic structure in direct proximity to the interface.

However, the antiferromagnetic (AFM) bulk presents a central ingredient for EB, which has been shown by the existence of a critical thickness, in experiments using ferromagnetic (FM)/AFM/FM trilayers[10,11] or diluted AFM materials.[12,13] Although these reports highlight contributions of the magnetic structure beyond the interface, the importance is far from being uniquely established and accepted.[14] For example, inserting magnetic or non-magnetic impurity layers at different locations away from the interface reveals that the effect can extent only up to few nm into the bulk.[15] Neutron scattering experiments indicated that the magnitude of EB is not influenced by the AFM domain size.[16]

In this Letter we have performed an experiment which is able to simultaneously detect and separate the contributions from all layers involved in EB. For this purpose, we employ post growth modification of the AFM at controlled depth under well-defined magnetic conditions. Contrary to previous studies, the present approach is insensitive to intrinsic morphologies, because the very same sample is modified, and therefore, all structural parameters and measurement protocols are identical. Therefore, we avoid issues related to different roughness,[17,18] grain size,[19–21] crystallinity,[22,23] interlayer diffusion,[24] and defects,[25,26] except for those intentionally introduced at pre-determined location within a single sample. Furthermore, we avoid altering the magnitude and sign of EB by different magnetic field history and cooling procedures.[27,28] Our observations demonstrate that the bulk of the AFM is crucial for establishing the EB.

In particular, we investigate the contribution of AFM bulk by controlled defect creation using light-ion bombardment. The impinging ions create defects whose location depends on the energy and dose of the ions.[29] In order to investigate defects preferentially created in the AFM, the FM layer is located below the AFM layer. The penetration depth of ions, and therefore the depth at which defect formation takes place, is controlled by varying Au capping layer thicknesses.[30] This approach is different to dilution during growth, since well-defined measurements are obtained with and without induced defects within the very same sample. Direct comparison of the EB before and after the bombardment as a function of Au thickness enables a separation of the magnetic contribution of interfacial and bulk defects.

Several sets of FM/AFM (Ni (10 nm)/FeF_2 (70 nm)) bilayers with constant thickness were grown simultaneously by electron-beam evaporation on (0001) Al_2O_3 substrates. Substrates were heated to 500 °C for 1 h prior to deposition, and then cooled to Ni growth temperature (~150 °C). The temperature was again increased (10 °C/min.) and kept at ~300 °C during FeF_2 deposition. The Au capping layer was deposited at room temperature. By using a shadow mask with translational movement, the samples were exposed to Au for different times, leading to a controlled variation of the Au thickness (Figure 1(b), inset). The base pressure remained below 10^{-6} Torr during the deposition of all layers. The Ni thickness of 10 nm was chosen after studying a range of FM thicknesses (within 5 to 35 nm of Ni in more than 50 samples) in order to obtain a fully biased hysteresis loop. The thickness

[a)]Author to whom correspondence should be addressed. Electronic mail: abasaran@ucsd.edu

 © 2014 AIP Publishing LLC

This article is copyrighted as indicated in the article. Reuse of AIP content is subject to the terms at: http://scitation.aip.org/termsconditions. Downloaded to IP: 128.54.23.18 On: Mon, 18 Aug 2014 14:14:58

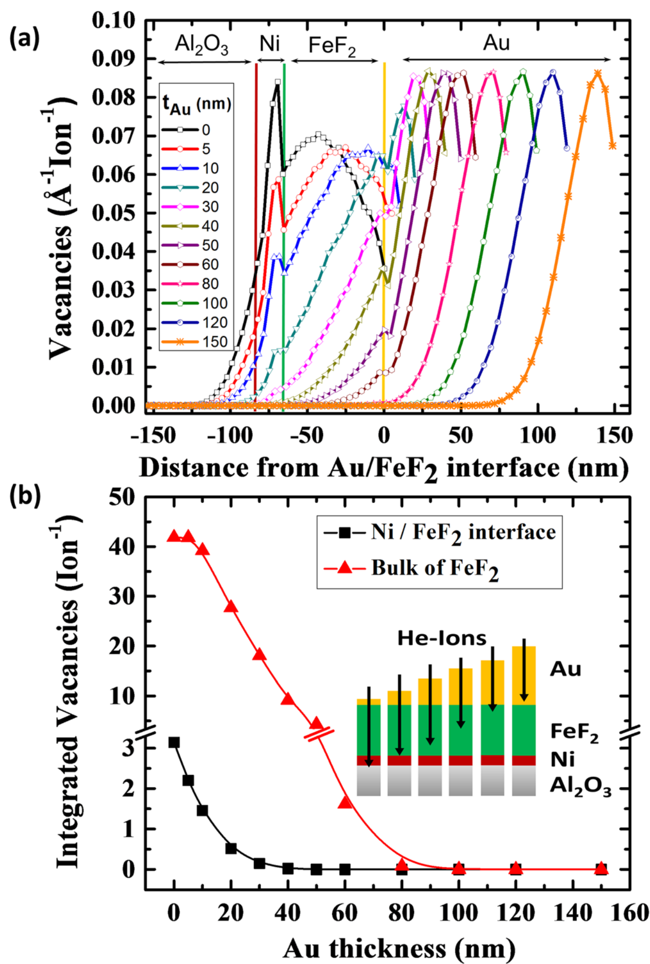

FIG. 1. (a) SRIM simulation of vacancy creation per ion and Å as a function of Au thickness. (b) Number of vacancies from (a) integrated over the interface (black squares) and FeF_2 thickness (red triangles). Above 80 nm (±10 nm) Au, no penetration of ions into AFM layer takes place. The FM/AFM interface is only affected up to 40 nm (±5 nm) Au. Inset: Schematic sample structure with varying Au thickness between samples.

of FeF_2 was chosen to be 70 nm, which is thicker than the typical AFM domain size of FeF_2 (~30 nm).[16]

All samples were investigated using vibrating sample magnetometry (VSM) and superconducting quantum interference device (SQUID) magnetometry, as well as x-ray diffraction and reflectometry in order to determine the structure. Following the initial structural and magnetic investigation, all samples were bombarded with He ions using a fixed 9 kV acceleration voltage in a home built setup[31] at a current of 300 nA. The acceleration voltage was chosen based on SRIM (Stopping and Range of Ions in Matter)[32] simulations to obtain an ion penetration into the FM layer for thin Au. The ion bombardment was carried out at a base pressure of 2.5×10^{-6} Torr at room temperature, i.e., well above the Néel temperature of FeF_2 ($T_N = 79$ K). A constant ion dose across the sample was achieved by defocussing of the beam by an electrostatic Einzel-lens and feeding it through an aperture. This leads to a beam spot of $2.5 \times 2.5\,mm^2$, which was scanned over the samples in lines. The centers of adjacent lines were displaced by 250 μm. The exposure time of the samples to the ion beam was controlled for each line to reach a total dose of 10^{15} ions/cm^2. The stopping range of the ions is solely determined by the Au layer thickness (t_{Au}).

The depth profile of the created vacancies obtained from SRIM simulations for different Au thicknesses is shown in Figure 1(a). Vertical lines indicate the location of the film interfaces with respect to the Au/FeF_2 interface at nominal zero. Figure 1(b) shows the total number of vacancies in the AFM bulk and at the FM/AFM interface obtained by integration of the simulations in the corresponding region. For this, the Ni/FeF_2 interface width was assumed to be 4 nm, which amounts three times the laterally averaged Gaussian interface profile determined by X-ray reflectometry (XRR). No vacancies are created at the Ni/FeF_2 interface above Au thicknesses of 40 nm (±5 nm), while defects in the AFM bulk can be anticipated up to $t_{Au} = 80$ nm (±10 nm).

X-ray diffraction (XRD) measurements reveal textured FeF_2 with (110) aligned with the surface normal. No change in crystalline orientation or diffraction profile was observed after the bombardment. Figure 2(a) shows XRR measurement and fit of the sample with 50 nm Au capping before and after the bombardment. The fitting was performed using MOTOFIT,[33] designed to fit slab models to a range of datasets with the same initial parameter set. The FM/AFM interface has the lowest roughness of the structure, shown in Figure 2(b). Typical differences in the reflectivity profiles of as grown and bombarded samples are on the scale shown in the inset of Figure 2(a). The deviations are well accounted for by only minor adjustments of structural parameters by

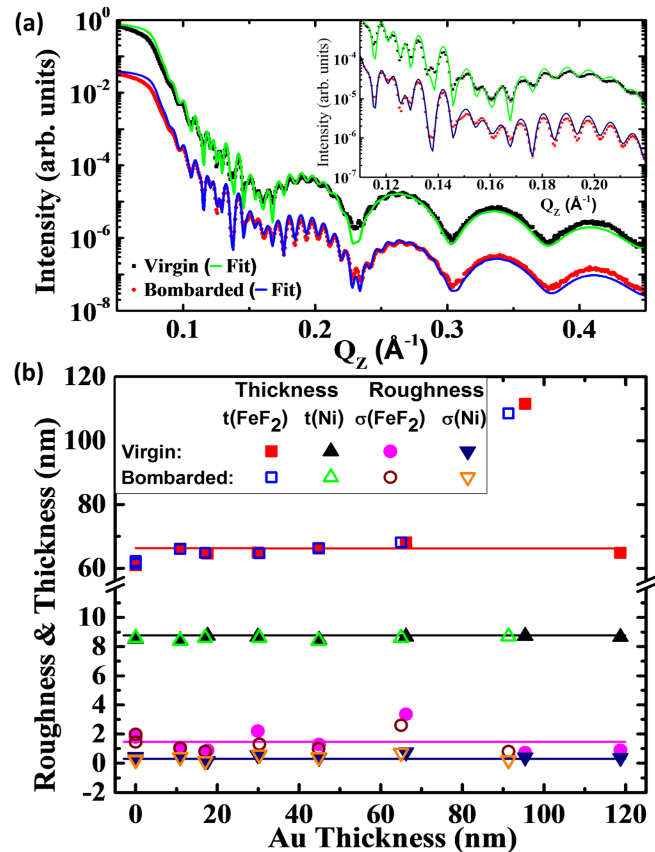

FIG. 2. (a) Example XRR measurement (symbols) for $t_{Au} = 50$ nm before and after bombardment and fit (lines). Inset: Enlarged view of the differences in the reflectivities due to the bombardment. The data are vertically shifted for clarity in both plots. (b) Layer thickness and roughness parameter obtained from XRR fits. FeF_2 and Ni parameters are plotted over the fitted Au thickness. Lines in (b) are guide to the eye.

This article is copyrighted as indicated in the article. Reuse of AIP content is subject to the terms at: http://scitation.aip.org/termsconditions. Downloaded to IP: 128.54.23.18 On: Mon, 18 Aug 2014 14:14:58

few angstroms (Figure 2(b)). We observe no structural changes in either interface roughness or sample structure due to the bombardment. The Ni (FeF_2) layer thickness shows a ± 0.2 nm (±4 nm) variation from sample to sample. The deviation from the nominal layer thicknesses amounts less than 10% for all samples, except of the sample with 100 nm Au capping. This can be related to a large uncertainty in the fitting for this particular thickness combination only.

For the magnetic characterizations, the following experimental protocol was fixed for all samples for consistency. A + 200 mT magnetic field was applied parallel to the film plane at 200 K, above the Néel temperature of FeF_2. This establishes fully reproducible magnetic initial conditions. The field was decreased to +20 mT, which was determined strong enough to keep the Ni saturated during cooling to measurement temperature. On the other hand, the cooling field was chosen low enough in order not to induce positive EB, which arises at higher cooling fields.[27,34] Hysteresis loops were recorded scanning the magnetic field starting from positive to negative saturation direction. The data have been corrected for a linear diamagnetic slope from the substrate. Magnetization values for all samples are consistent within 2% and normalized to the maximum value at saturation. Although samples are grown simultaneously, differences in the Ni volume or different domain formation in the AFM layer can arise and explain the variation. The contribution of magnetic moments from free Fe can also differ from sample to sample. EB is determined for each sample individually by the offset of the loop center along the applied field axis. Only temperatures well below the Néel temperature of FeF_2 are considered. No training effect was observed. Differences in EB between samples are excluded from the discussion by normalizing the change in EB field (ΔH_{EB}) due to bombardment to the value before the bombardment (H^{v}_{EB}).

Figure 3 shows typical magnetic hysteresis loops at 20 K of the sample with 60 nm Au capping layer before and after the ion bombardment. A shift of $H^{v}_{EB} = 21$ mT was recorded before the bombardment, which decreased to $H^{b}_{EB} = 17$ mT after the bombardment. This corresponds to a decrease of $\Delta H_{EB}/H^{v}_{EB} = (H^{v}_{EB} - H^{b}_{EB})/H^{v}_{EB} = 18\%$ for this sample. H^{v}_{EB} and H^{b}_{EB} refer to EB fields for the virgin and bombarded sample, respectively.

The relative change $\Delta H_{EB}/H^{v}_{EB}$ as a function of Au thickness is summarized in Figure 4. This plot includes 18 samples deposited in 3 different sets. Each set comprises thick and thin Au layers. Two sets were measured with VSM (black squares and red circles) at 20 K, and one set was measured in a SQUID magnetometer (blue triangles) at 10 K. Experimental errors of 10% were estimated based on sample mounting and diamagnetic background corrections. The vertical lines mark the regions affected by ion bombardment extracted from Figure 1. Without capping layer, the initial decrease of H_{EB} amounts to 20%. With increasing Au thickness, the change shows a peak of 35% at $t_{Au} = 20$–30 nm. Beyond $t_{Au} = 40$ nm, a plateau at 20% is observed over 40 nm. Above $t_{Au} = 80$ nm, the change gradually vanishes. Both, VSM and SQUID measurements show a good agreement in this behavior. Therefore, the observed effect is not related to a single deposition condition. Small quantitative discrepancies between individual thicknesses are related to the natural variation between samples grown as different sets with slightly different conditions.

The observation of a finite change in $\Delta H_{EB}/H^{v}_{EB}$ well above $t_{Au} = 40$ nm shows that the bulk of the AFM layer must have an influence on EB. According to the SRIM simulations, no defects are created at or near the FM/AFM interface above this critical thickness (green line in Figure 4). Only the defect creation in the bulk extends to $t_{Au} = 80$ nm, which agrees with the observed plateau of $\Delta H_{EB}/H^{v}_{EB}$. Above $t_{Au} = 80$ nm (yellow line in Figure 4), ions do not penetrate through the Au, and therefore, no defects should be created in FeF_2. The residual change observed above 80 nm in some samples arises from an uncertainty in the Au thickness, an experimental uncertainty in the radiation damage

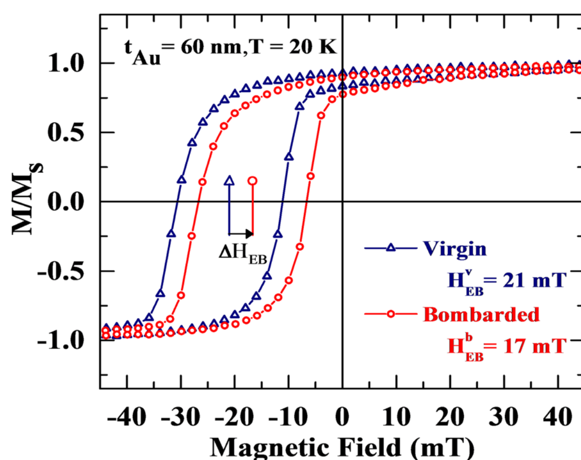

FIG. 3. Example of a VSM magnetic hysteresis for as-grown (blue triangles) and bombarded (red circles) sample with $t_{Au} = 60$ nm. Both curves are obtained at 20 K after 20 mT field cooling from 200 K. The He-ion bombardment decreases the loop shift by 18%. The magnetization values are normalized to saturation.

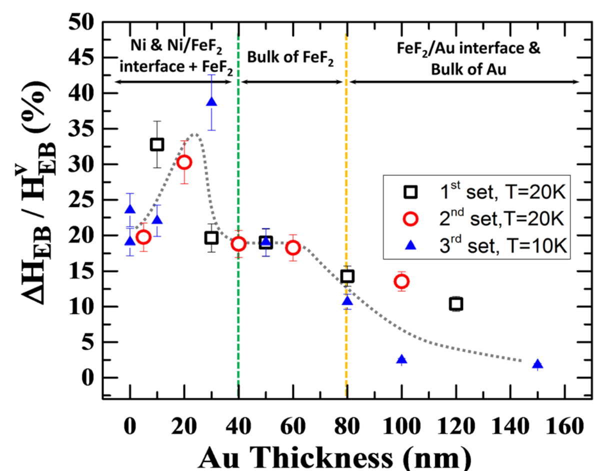

FIG. 4. Relative change of EB field as a function of the Au thickness for three sets of samples. Sets one and two were measured with VSM at 20 K (black open squares and red open circles, respectively). The third set (blue triangles) was measured with SQUID magnetometer at 10 K. Vertical green and yellow dashed lines obtained from Figure 1 indicate separation of affected regions due to bombardment. The gray dashed line is a guide to the eye. We should point out that there are two data points overlapping at 50 nm Au from two different data sets showing reproducibility between measurement. Note the apparent slower change as a function of thickness for samples measured with VSM at higher Au thicknesses.

This article is copyrighted as indicated in the article. Reuse of AIP content is subject to the terms at: http://scitation.aip.org/termsconditions. Downloaded to IP: 128.54.23.18 On: Mon, 18 Aug 2014 14:14:58

and an uncertainty of the penetration depth from SRIM simulations. This adds to the error bars of the data points and leads to error bars along the x-axis, which are not included since they are not systematic and not accessible. The observation of the AFM bulk affecting H_{EB} is independent of the detailed mechanism leading to the change in H_{EB}. Since the bombardment took place well above the Néel temperature and measurement protocols are kept the same, time and temperature dependent effects[35,36] or changes in the frozen in AFM structure[37] can be neglected. The result is independent of the microscopic or macroscopic sample morphology since only the Au layer is used to determine the ion penetration depth and, therefore, the damage profile. In addition, the damage is low enough not to be detected by XRR and XRD.

The influence of the AFM bulk on EB is further supported considering the length scales in the experiment. For Au thicknesses which include a defect creation at the interface in addition to the FeF_2 bulk, $\Delta H_{EB}/H^v_{EB}$ peaks at 35%. The width of this interface related maximum is 20 nm. The plateau immediately after the peak extends for 50 nm at a change of $\Delta H_{EB}/H^v_{EB} = 20\%$. Such a constant EB reduction over almost three times the peak width is unlikely even considering an asymmetric damage profile of the interface. Consequently, the plateau in $\Delta H_{EB}/H^v_{EB}$ is only explained by contributions from the bulk of the AFM.

A detailed discussion of the change in EB with defect creation by ion bombardment should consider the individual regions and possible mechanisms. We observe that defects created in the AFM bulk decrease the magnitude of H_{EB}. This can be related to a diminished AFM order and reduced AFM anisotropy, which can lead to an increased number of freely rotatable Fe moments. These moments no longer contribute to the density of pinned uncompensated moments, which further decreases H_{EB}.[16,38–40] In addition, this reduces the AFM domain size, which was reported to decrease the EB in $Fe_xZn_{1-x}F_2$.[41] We note that according to the domain state model,[13,42] H_{EB} increases with the number of uncompensated moments, which has been experimentally supported by measurements of $Co_xMg_{1-x}O$[13,42] and $Fe_xZn_{1-x}F_2$.[43,44] This does not contradict our results but highlights that EB crucially depends on the type of defect created, i.e., pinned or unpinned uncompensated magnetization. The existence of uncompensated magnetization in the AFM bulk[40,45] and intrinsic effects[46] has been shown previously, but our results unambiguously show contributions to the EB.

Below $t_{Au} = 40$ nm, defect creation in the AFM bulk, at the AFM/FM interface and in the FM needs to be taken into account simultaneously. Within the FM layer, defects alter the magnetic domain structure, leading to pinning sites for FM domains.[47] In our experiments, the coercivity remains the same after the bombardment. On the other hand, an enhanced coercivity upon ion bombardment was observed for FeMn/FeNi EB system,[48] but not for NiO/FeNi[35] and, therefore, appears to depend on the specific sample morphology. It has recently been shown that the lateral and in-depth domain landscape of the FM strongly influences the EB.[34,49] Previous studies on FeF_2 show a decrease of H_{EB} with increasing interface roughness.[22] In our study, XRR shows that within our resolution, the chemical profiles are unaltered by bombardment on sub-nm length scales. In contrast, magnetic defects near the interface increase the area density of uncompensated moments. This is expected to enhance H_{EB}.[9,38] Therefore, the balance between enhancement and decrease of H_{EB} is complex and is expected to highly depend on the ratio between defects in the FM, interface, and AFM bulk. Independent of all possible scenarios, the AFM bulk has to be considered to explain all experimental observations.

In summary, we have shown that the AFM bulk has a direct influence on the absolute magnitude of EB. The location of defects created by light-ion bombardment has been controlled by varying the thickness of an inert Au capping layer. A change in EB is observed with defects only formed in the FeF_2 bulk, at Au thicknesses where the interface is unaffected. A maximum change of EB is observed if defects are created throughout the bulk of AFM layer and at the FM/AFM interface. This can be attributed to a balance of several mechanisms for which both bulk and interface need to be considered. The importance of the AFM bulk for determining EB is independent of these complex scenarios.

We thank Professors G. Güntherodt, X. Battle, and R. Morales for fruitful discussions. This is a highly collaborative research. The experiments were conceived jointly, the data were extensively debated, and the paper was written by multiple iterations between all the coauthors. Samples were fabricated, characterized, and measured at UCSD. The research at UCSD was supported by the Office of Basic Energy Science, U.S. Department of Energy, BES-DMS funded by the Department of Energy's Office of Basic Energy Science, DMR under Grant No. DE FG03 87ER-45332. H.H. thanks J. F. Ziegler for useful discussions and support on SRIM.

[1]C. Tsang, J. Appl. Phys. **55**(6), 2226 (1984).
[2]B. Negulescu, D. Lacour, F. Montaigne, A. Gerken, J. Paul, V. Spetter, J. Marien, C. Duret, and M. Hehn, Appl. Phys. Lett. **95**(11), 112502 (2009).
[3]S. S. P. Parkin, K. P. Roche, M. G. Samant, P. M. Rice, R. B. Beyers, R. E. Scheuerlein, E. J. O'Sullivan, S. L. Brown, J. Bucchigano, D. W. Abraham, Y. Lu, M. Rooks, P. L. Trouilloud, R. A. Wanner, and W. J. Gallagher, J. Appl. Phys. **85**(8), 5828 (1999).
[4]X. Chen, A. Hochstrat, P. Borisov, and W. Kleemann, Appl. Phys. Lett. **89**(20) 202508 (2006).
[5]C. Binek, A. Hochstrat, X. Chen, P. Borisov, W. Kleemann, and B. Doudin, J. Appl. Phys. **97**(10), 10C514 (2005).
[6]R. Morales, M. Kovylina, I. K. Schuller, A. Labarta, and X. Batlle, Appl. Phys. Lett. **104**(3), 032401 (2014).
[7]W. H. Meiklejohn and C. P. Bean, Phys. Rev. **102**(5), 1413 (1956).
[8]J. Nogués and I. K. Schuller, J. Magn. Magn. Mater. **192**(2), 203 (1999).
[9]A. E. Berkowitz and K. Takano, J. Magn. Magn. Mater. **200**(1–3), 552 (1999).
[10]R. Morales, Z.-P. Li, J. Olamit, K. Liu, J. M. Alameda, and I. K. Schuller, Phys. Rev. Lett. **102**(9), 097201 (2009).
[11]D. N. H. Nam, W. Chen, K. G. West, D. M. Kirkwood, J. Lu, and S. A. Wolf, Appl. Phys. Lett. **93**(15), 152504 (2008).
[12]P. Miltényi, M. Gierlings, J. Keller, B. Beschoten, G. Güntherodt, U. Nowak, and K. D. Usadel, Phys. Rev. Lett. **84**(18), 4224 (2000).
[13]J. Keller, P. Miltényi, B. Beschoten, G. Güntherodt, U. Nowak, and K. D. Usadel, Phys. Rev. B **66**(1), 014431 (2002).
[14]P. K. Manna and S. M. Yusuf, Phys. Rep. **535**(2), 61 (2014).
[15]M. Ali, C. H. Marrows, and B. J. Hickey, Phys. Rev. B **77**(13), 134401 (2008).
[16]M. R. Fitzsimmons, D. Lederman, M. Cheon, H. Shi, J. Olamit, I. V. Roshchin, and I. K. Schuller, Phys. Rev. B **77**(22), 224406 (2008).
[17]W. Kuch, L. I. Chelaru, F. Offi, J. Wang, M. Kotsugi, and J. Kirschner, Nat. Mater. **5**(2), 128–133 (2006).
[18]J. Nogués, D. Lederman, T. J. Moran, I. K. Schuller, and K. V. Rao, Appl. Phys. Lett. **68**(22), 3186 (1996).

This article is copyrighted as indicated in the article. Reuse of AIP content is subject to the terms at: http://scitation.aip.org/termsconditions. Downloaded to IP: 128.54.23.18 On: Mon, 18 Aug 2014 14:14:58

[19]T. Saerbeck, H. Zhu, D. Lott, H. Lee, P. R. LeClair, G. J. Mankey, A. P. J. Stampfl, and F. Klose, J. Appl. Phys. **114**(1), 013901 (2013).
[20]K. Nishioka, C. Hou, H. Fujiwara, and R. D. Metzger, J. Appl. Phys. **80**(8), 4528 (1996).
[21]M. Pakala, Y. Huai, G. Anderson, and L. Miloslavsky, J. Appl. Phys. **87**(9), 6653 (2000).
[22]J. Nogués, T. J. Moran, D. Lederman, I. K. Schuller, and K. V. Rao, Phys. Rev. B **59**(10), 6984 (1999).
[23]R. Jungblut, R. Coehoorn, M. T. Johnson, J. aan de Stegge, and A. Reinders, J. Appl. Phys. **75**(10), 6659 (1994).
[24]Y. K. Kim, S.-R. Lee, S. A. Song, G.-S. Park, H. S. Yang, and K.-I. Min, J. Appl. Phys. **89**(11), 6907 (2001).
[25]A. Mougin, T. Mewes, M. Jung, D. Engel, A. Ehresmann, H. Schmoranzer, J. Fassbender, and B. Hillebrands, Phys. Rev. B **63**(6), 060409 (2001).
[26]J.-V. Kim and R. L. Stamps, Appl. Phys. Lett. **79**(17), 2785 (2001).
[27]J. Nogués, D. Lederman, T. J. Moran, and I. K. Schuller, Phys. Rev. Lett. **76**(24), 4624 (1996).
[28]Z.-P. Li, J. Eisenmenger, C. W. Miller, and I. K. Schuller, Phys. Rev. Lett. **96**(13), 137201 (2006).
[29]T. Mewes, R. Lopusnik, J. Fassbender, B. Hillebrands, M. Jung, D. Engel, A. Ehresmann, and H. Schmoranzer, Appl. Phys. Lett. **76**(8), 1057 (2000).
[30]M. Urbaniak, P. Kuświk, Z. Kurant, M. Tekielak, D. Engel, D. Lengemann, B. Szymański, M. Schmidt, J. Aleksiejew, A. Maziewski, A. Ehresmann, and F. Stobiecki, Phys. Rev. Lett. **105**(6), 067202 (2010).
[31]D. Lengemann, D. Engel, and A. Ehresmann, Rev. Sci. Instrum. **83**(5), 053303 (2012).
[32]J. Ziegler and J. Biersack, in *Treatise on Heavy-Ion Science*, edited by D. Allan Bromley (Springer US, 1985), pp. 93.
[33]A. Nelson, J. Appl. Crystallogr. **39**(2), 273 (2006).
[34]M. Kovylina, R. Morales, A. Labarta, and X. Batlle, Phys. Rev. B **86**(22), 224414 (2012).
[35]A. Ehresmann, D. Junk, D. Engel, A. Paetzold, and K. Röll, J. Phys. D: Appl. Phys. **38**(6), 801 (2005).
[36]A. Ehresmann, C. Schmidt, T. Weis, and D. Engel, J. Appl. Phys. **109**(2), 023910 (2011).
[37]A. Ehresmann, D. Engel, T. Weis, A. Schindler, D. Junk, J. Schmalhorst, V. Höink, M. D. Sacher, and G. Reiss, Phys. Status Solidi B **243**(1), 29 (2006).
[38]J.-I. Hong, T. Leo, D. J. Smith, and A. E. Berkowitz, Phys. Rev. Lett. **96**(11), 117204 (2006).
[39]S. Brück, G. Schütz, E. Goering, X. Ji, and K. M. Krishnan, Phys. Rev. Lett. **101**(12), 126402 (2008).
[40]S. Roy, M. R. Fitzsimmons, S. Park, M. Dorn, O. Petracic, I. V. Roshchin, Z.-P. Li, X. Batlle, R. Morales, A. Misra, X. Zhang, K. Chesnel, J. B. Kortright, S. K. Sinha, and I. K. Schuller, Phys. Rev. Lett. **95**(4), 047201 (2005).
[41]H. Shi, Z. Liu, and D. Lederman, Phys. Rev. B **72**(22), 224417 (2005).
[42]U. Nowak, K. D. Usadel, J. Keller, P. Miltényi, B. Beschoten, and G. Güntherodt, Phys. Rev. B **66**(1), 014430 (2002).
[43]H. Shi, D. Lederman, and E. E. Fullerton, J. Appl. Phys. **91**(10), 7763 (2002).
[44]H. Shi, D. Lederman, N. R. Dilley, R. C. Black, J. Diedrichs, K. Jensen, and M. B. Simmonds, J. Appl. Phys. **93**(10), 8600 (2003).
[45]M. R. Fitzsimmons, B. J. Kirby, S. Roy, Z.-P. Li, I. V. Roshchin, S. K. Sinha, and I. K. Schuller, Phys. Rev. B **75**(21), 214412 (2007).
[46]D. Kaya, P. N. Lapa, P. Jayathilaka, H. Kirby, C. W. Miller, and I. V. Roshchin, J. Appl. Phys. **113**(17), 17D717 (2013).
[47]K. D. Usadel and R. L. Stamps, Phys. Rev. B **82**(9), 094432 (2010).
[48]J. Juraszek, J. Fassbender, S. Poppe, T. Mewes, B. Hillebrands, D. Engel, A. Kronenberger, A. Ehresmann, and H. Schmoranzer, J. Appl. Phys. **91**(10), 6896 (2002).
[49]R. Morales, Z.-P. Li, O. Petracic, X. Batlle, I. K. Schuller, J. Olamit, and K. Liu, Appl. Phys. Lett. **89**(7), 072504 (2006).

This article is copyrighted as indicated in the article. Reuse of AIP content is subject to the terms at: http://scitation.aip.org/termsconditions. Downloaded to IP: 128.54.23.18 On: Mon, 18 Aug 2014 14:14:58